

# Green Synthesis, Characterization and Bioactivity of AuNPs from *E. cardamomum*: A Comparative Study

Sowmya KM, Narendhirakannan RT\*

Department of Biochemistry, Kongunadu Arts and Science College (Autonomous), G.N. Mills P.O, Coimbatore, Tamil Nadu, INDIA.

## ABSTRACT

**Background:** Nanoparticles, particularly those from natural sources like *E. cardamomum*, have garnered significant interest due to their unique physicochemical characteristics and potential applications in medicine. **Materials and Methods:** This study explores the synthesis and characterization of Gold Nanoparticles (AuNPs) synthesized from *E. cardamomum*, focusing on their antibacterial, antioxidant and anti-inflammatory properties. **Results and Discussion:** The green synthesis approach using extracts from cardamom seeds and pods facilitated the production of spherical AuNPs, confirmed by UV-vis spectroscopy, SEM, TEM, XRD, EDX and FTIR analysis. Comparative analysis revealed that AuNPs synthesized from cardamom pods exhibited superior antibacterial, antioxidant and anti-inflammatory activities compared to those from seeds. Antibacterial efficacy was evaluated through well-diffusion and MIC methods, highlighting concentration-dependent effects. Various antioxidant assays, including DPPH scavenging and FRAP, demonstrated potent radical scavenging capabilities. Additionally, assays for anti-inflammatory properties, such as albumin denaturation and hemolysis inhibition, underscored the nanoparticles' potential in mitigating inflammatory responses. **Conclusion:** These findings underscore the therapeutic potential of AuNPs of *E. cardamomum* pods, suggesting their promise as lead candidates for developing novel treatments targeting microbial infections and oxidative stress-related conditions. This research contributes valuable insights into harnessing plant-mediated nanoparticles for medicinal applications, emphasizing their role in advancing pharmaceutical and biomedical sciences.

**Keywords:** Antioxidant, Anti-inflammatory, *E. cardamomum*, AuNPs, Nanoparticles.

## Correspondence:

**Dr. Narendhirakannan R.T**

Assistant Professor, Department of Biochemistry, Kongunadu Arts and Science College (Autonomous), G.N. Mills P.O, Coimbatore, Tamil Nadu, INDIA.  
Email: rtnaren@kongunaducollege.ac.in

**Received:** 31-07-2024;

**Revised:** 12-11-2024;

**Accepted:** 09-01-2025.

## INTRODUCTION

Nanotechnology encompasses a broad interdisciplinary field focused on creating innovative nanostructures up to 100 nm in size, where properties such as particle size, shape and distribution play crucial roles (Sahu *et al.*, 2023). Nanoparticles at this scale exhibit unique characteristics including electron density configuration, thermal conductivity, optical properties and magnetic behavior (Modena *et al.*, 2019). Extensive research has illuminated diverse applications of nanoparticles in biomedicine, pharmaceuticals, drug delivery, cosmetics and catalysis (Zahin *et al.*, 2020). Nanotherapeutics are increasingly seen as promising solutions to address challenges in drug delivery systems, including solubility, targeting, bio-distribution, bioavailability and therapeutic efficacy (Muniyappan *et al.*, 2021).

Recent attention has focused on Gold Nanoparticles (AuNPs) due to their distinct physicochemical properties and versatile applications (Herizchi *et al.*, 2016). Among metallic nanoparticles, AuNPs can interact with light through Surface Plasmon Resonance (SPR) (Yoganandham *et al.*, 2018). However, conventional chemical synthesis methods often produce hazardous by-products that pose risks to human health (Dikshit *et al.*, 2021), highlighting the need for eco-friendly nanoparticle synthesis approaches within nanotechnology (Kumar *et al.*, 2021).

Utilizing plants for nanoparticle synthesis presents a sustainable alternative to chemical methods, offering scalability and environmental benefits (Saratale *et al.*, 2018). Plant extracts serve as efficient reducing and capping agents in nanoparticle synthesis due to their rich phytochemical content (Patil and Chandrasekaran, 2020). *E. cardamomum*, commonly known as Cardamom, is a fragrant spice with significant medicinal value and cultural importance (Bano *et al.*, 2016). This study focuses on synthesizing AuNPs from different parts of cardamom seeds and pods using green synthesis methods, while evaluating their antibacterial, antioxidant and anti-inflammatory properties.



DOI: 10.5530/ijpi.20250039

### Copyright Information :

Copyright Author (s) 2025 Distributed under Creative Commons CC-BY 4.0

Publishing Partner : Manuscript Technomedia. [www.mstechnomedia.com]

## MATERIALS AND METHODS

### Acquisition of plant material and extract preparation

The seeds and pods of *E. cardamomum* were obtained from Idukki and underwent separate shade drying processes before being finely ground using a mechanical grinder. The resulting powders were stored in sealed containers. To prepare the aqueous extract, 2g of powdered samples from both pods and seeds were individually mixed with 20 mL of deionized water. This mixture was heated under controlled conditions, maintaining a temperature between 70-80°C, for 1 hr to facilitate extraction. After this step, the solution was centrifuged at 5000 rpm for 15 min to remove any insoluble residues and obtain a clear aqueous extract. This extract, containing bioactive compounds from *E. cardamomum*, was then used as the bio reductant in the synthesis of AuNPs (Pattanayak and Nayak, 2013).

### Synthesis of AuNPs

Initially, a 20 mL aqueous solution of HAuCl<sub>4</sub> was prepared with a concentration of 1 mM. Following this, 2 mL portions of the extracts from both pods and seeds were individually added to the prepared HAuCl<sub>4</sub> solution. These mixtures were then incubated under controlled conditions at temperatures between 40-60°C for 15 min. Over the course of this incubation, the emergence of a noticeable violet coloration in the reaction mixtures indicated the synthesis of nanoparticles visually (Pattanayak and Nayak, 2013).

### Characterization of Nanoparticles

#### UV-vis Spectra analysis

To assess the reduction of Au<sup>3+</sup> salts to nanoparticles, the UV-vis absorption spectra of the extracts from seeds and pods were examined using a UV-vis Spectrophotometer from Shimadzu Corporation, Japan. This analysis was conducted across a wavelength range of 300 nm to 800 nm. Following this initial analysis, samples from the reaction mixtures containing the synthesized nanoparticles were also analyzed using UV-vis spectroscopy. The absorption spectra obtained from these analyses provided critical information about nanoparticle formation, revealing characteristic absorption peaks within the specified wavelength range. By comparing the absorption spectra of the seed and pod extracts before and after the reduction process, any shifts or changes in peak intensity indicative of nanoparticle formation.

#### X-ray Diffraction (XRD) studies

AuNPs synthesized from extracts of both seeds and pods of *E. cardamomum* were characterized using XRD analysis. XRD patterns were obtained using a Rigaku Miniflex 600 X-ray diffractometer (Japan), employing Cu K $\alpha$  radiation ( $\lambda=1.5406$  Å). The measurements were conducted at room temperature over a 2 $\theta$  range of 10-80° with a step size of 0.02°. The XRD patterns

obtained were analyzed to gain insights into the crystalline structure of the synthesized nanoparticles. Furthermore, the average size of the nanoparticles was determined using the Debye-Scherrer equation:  $D=k\lambda/\beta\cos\theta$ .

Where D is the average size of the nanoparticles, k is a constant (typically 0.9),  $\lambda$  is the wavelength of the X-ray radiation,  $\beta$  is the Full Width at Half Maximum (FWHM) of the XRD peak and  $\theta$  is the Bragg angle. This equation allowed for the calculation of nanoparticle size based on the XRD data.

#### Fourier Transform Infrared (FTIR) Spectroscopy analysis

FTIR analysis was performed using a SHIMADZU IR Spirit instrument (Japan). Transmittance spectra were recorded across the wave number range of 4000-600 cm<sup>-1</sup> at a resolution of 16 cm<sup>-1</sup>. This approach facilitated a comprehensive investigation of the functional groups within samples synthesized from *E. cardamomum* seed and pod extracts. The FTIR analysis involved examining absorption peaks and their respective wave numbers to gain critical insights into the chemical composition and molecular structure of the extracted compounds.

#### Scanning Electron Microscopy (SEM) analysis

SEM was employed to assess the morphological characteristics of the synthesized AuNPs. The examination was conducted using a Carl Zeiss instrument from Germany. Samples for SEM analysis were prepared using standard techniques, where a thin layer of the nanoparticle dispersion was deposited onto a suitable substrate. These prepared samples were then subjected to SEM imaging under appropriate operational conditions and magnifications. SEM analysis provided high-resolution visualization of the shape, size and distribution of the AuNPs produced from *E. cardamomum* seed and pod extracts.

#### Energy-Dispersive X-Ray (EDX) analysis

EDX was utilized to analyze the elemental composition of AuNPs synthesized from extracts of both seeds and pods of *E. cardamomum*. The EDX measurement was performed using an EDS X-ray spectrophotometer integrated with the SEM instrument (ZEISS EVO) from Oxford Instruments, United Kingdom. During the EDX analysis, X-ray spectra emitted from the sample surface upon electron beam excitation were captured. This technique enabled both qualitative and quantitative assessment of the elemental constituents present within the synthesized nanoparticles.

#### TEM and particle size analysis

TEM analysis was conducted to examine the morphology, size and distribution of AuNPs synthesized from extracts of *E. cardamomum* seeds and pods. TEM samples were prepared by

depositing a drop of the nanoparticle solution onto a grid and allowing it to air dry at room temperature.

The dried grids were then analyzed using a JEOL 2000 FX-II TEM microscope from Japan at the appropriate magnification settings. This approach enabled high-resolution imaging and detailed observation of individual nanoparticles. Additionally, Selected Area Electron Diffraction (SAED) was employed during TEM analysis to investigate the crystalline structure of the nanoparticles. SAED provided valuable insights into the crystallographic orientation and atomic arrangement within the synthesized nanoparticles.

### Anti-Bacterial Activity

The anti-bacterial activity was carried out using three different multi-drug resistant strains such as *Escherichia coli*, *Klebsiella pneumoniae* and *Staphylococcus aureus*. All of the test organisms were received from the Genolites Research and Development Laboratory in Coimbatore. The test organisms were kept at 4°C in Mueller-Hinton Agar and sub cultured once a month.

The antibacterial activity of *E. cardamomum* seed and pod mediated nanoparticles was evaluated using standard microbiological techniques. Initially, Mueller Hinton agar plates were prepared and inoculated with an overnight culture of test organisms including *Escherichia coli*, *Klebsiella pneumoniae* and *Staphylococcus aureus* at a concentration of  $5 \times 10^6$  colony-forming units per milliliter (cfu/mL). Wells of 6 mm diameter were made in the agar, into which 100 µL of the respective *E. cardamomum* seed and pod nanoparticles were introduced. Following incubation overnight, the plates were examined for zones of inhibition around the wells and the diameters of these zones were measured in millimeters to assess the antibacterial efficacy of the nanoparticles.

Subsequently, the nanoparticles that demonstrated significant inhibition zones were selected for further comparison with standard antibiotics using the disc diffusion method. Specifically, discs containing standard antibiotics such as cefmetazole (30 µg), ampicillin (10 µg), tetracycline (30 µg) and ciprofloxacin (5 µg) were placed on Mueller-Hinton agar plates previously seeded with the respective bacterial strains. Simultaneously, 100 µL of the selected nanoparticle suspension was introduced into a separate well (6 mm) on the agar surface. After overnight incubation, the diameters of the zones of inhibition around both the nanoparticle wells and antibiotic discs were measured to compare the antibacterial effectiveness of the nanoparticles with that of standard antibiotics against the test bacterial strains (Boggula *et al.*, 2017).

### Minimum Inhibitory Concentration (MIC)

MIC of *E. cardamomum* pod mediated AuNPs against various test bacterial strains was determined using the Resazurin method, following procedures outlined by Elshikh *et al.*, 2016.

Initially, 100 µL of *E. cardamomum* pod mediated AuNPs were added to the first row of a sterile 96-well microtiter plate, while 50 µL of nutrient broth was added to each subsequent well to facilitate serial dilutions. This created a gradient of decreasing nanoparticle concentrations across the plate. Subsequently, 50 µL of each dilution was inoculated with the respective test organisms at a concentration of  $5 \times 10^6$  cfu/mL, followed by the addition of 10 µL of Resazurin solution to each well. The microtiter plate was then loosely covered with cling film to prevent desiccation and was placed in an incubator set at 37°C overnight. Post-incubation, wells showing a color change from purple to pink indicated bacterial growth, with the MIC recorded as the lowest concentration of nanoparticles inhibiting this color change (Sarker *et al.*, 2007).

### Antioxidant Activity

The *in vitro* antioxidant activity of the AuNPs synthesized using seed and pod of *E. cardamomum* was determined using the following methods: DPPH (2,2-Diphenyl-1-Picrylhydrazyl) scavenging method, FRAP (Ferric ion Reducing Antioxidant Power) assay, Hydrogen peroxide scavenging assay, reducing power assay and phosphomolybdenum assay. Ascorbic acid was used as standard.

### DPPH (2,2-diphenyl-1-picrylhydrazyl) radical scavenging assay

The DPPH radical scavenging activity of AuNPs synthesized using aqueous extracts from seeds and pods of *E. cardamomum* was evaluated following the method outlined by Shimada *et al.*, 1992, Various concentrations (25, 50, 75, 100, 250, 500, 750 and 1000 µg/mL) of AuNPs synthesized from seed and pod extracts were prepared separately and combined with 3 mL of freshly prepared methanolic DPPH solution (0.1 mM). The mixture was then incubated at 37°C for 30 min, after which the absorbance was measured at 517 nm using a spectrophotometer. Each sample was analyzed in triplicate to ensure reliability and accuracy of the results.

$$\text{Inhibition (\%)} = \frac{\text{Absorbance of Control} - \text{Absorbance of Sample}}{\text{Absorbance of Control}} \times 100$$

### FRAP (Ferric ion Reducing Antioxidant Power) assay

FRAP assay was employed to assess the ability of AuNPs synthesized from aqueous extracts of *E. cardamomum* seed and pod to reduce  $\text{Fe}^{3+}$  ions to  $\text{Fe}^{2+}$  in the presence of 2,4,6-Tripyridyl-s-Triazine (TPTZ). Different concentrations (25, 50, 75, 100, 250, 500, 750 and 1000 µg/mL) of AuNPs synthesized from seed and pod extracts were prepared separately and mixed with 3 mL of FRAP reagent. The reaction mixture was incubated at 37°C for 10 min to facilitate the reduction reaction, after which the absorbance was measured at 593 nm using a UV-vis spectrophotometer (Guo *et al.*, 2003).

### Hydrogen peroxide scavenging activity

The Hydrogen peroxide (H<sub>2</sub>O<sub>2</sub>) scavenging activity of AuNPs synthesized from aqueous extracts of *E. cardamomum* seed and pod was evaluated following the methodology described by Sivakumar *et al.*, 2015, AuNPs at concentrations ranging from 25 to 1000 µg/mL were prepared separately and mixed with 2 mL of hydrogen peroxide solution (10 mM, pH 7.4). The mixtures were then incubated at 37°C for 10 min to allow the scavenging reaction to occur. After incubation, the absorbance of the reaction mixture was measured at 230 nm using a spectrophotometer.

$$\text{Inhibition (\%)} = \frac{\text{Absorbance of Control} - \text{Absorbance of Sample}}{\text{Absorbance of Control}} \times 100$$

### Reducing Power Assay

The Reducing Power Assay of AuNPs synthesized using aqueous extracts from seeds and pods of *E. cardamomum* was conducted following a modified protocol based on Sutharsingh *et al.*, 2011 AuNPs at concentrations ranging from 25 to 1000 µg/mL were prepared separately and mixed with 1 mL of phosphate buffer (1%) and 1 mL of potassium ferrocyanide (1%). The mixtures were then incubated at 50°C for 20 min to facilitate the reduction reaction. After incubation, 1 mL of trichloroacetic acid (10%) was added to each test tube, followed by centrifugation for 10 min. The supernatant (1.5 mL) was mixed with an equal volume of distilled water (1.5 mL) and 300 µL of 0.1% Ferric Chloride (FeCl<sub>3</sub>) was added. The absorbance of the resulting solution was measured at 700 nm using a spectrophotometer to determine the reducing power of AuNPs.

### Phosphomolybdenum Assay

The antioxidant activity of AuNPs synthesized from extracts of *E. cardamomum* seed and pod was assessed using the phosphomolybdenum assay as per the method outlined by Sahreen *et al.*, 2010, A reagent solution containing 0.6 M sulfuric acid, 28 mM sodium phosphate and 4 mM ammonium molybdate was prepared. Varying concentrations (25, 50, 75, 100, 250, 500, 750 and 1000 µg/mL) of synthesized AuNPs were separately added to 1 mL of the reagent solution. The reaction mixtures were incubated in a water bath at 95°C for 90 min and subsequently cooled to room temperature. The absorbance of each sample was measured at 765 nm using a UV-vis spectrophotometer to determine the total antioxidant capacity of the AuNPs.

$$\text{Inhibition (\%)} = \frac{\text{Absorbance of Control} - \text{Absorbance of Sample}}{\text{Absorbance of Control}} \times 100$$

### Anti-Inflammatory Activity

The *in vitro* anti-inflammatory activity of the AuNPs synthesized from seed and pod of *E. cardamomum* was examined by the albumin denaturation method and heat-induced hemolysis method. Aspirin was used as standard.

### Albumin denaturation method

The albumin denaturation assay was conducted following the protocol adapted from Govindappa *et al.*, 2018, with minor changes. The reaction mixture included 3 mL of 5% aqueous bovine albumin solution and varying concentrations of AuNPs synthesized from seed and pod extracts of *E. cardamomum*. The test tubes were first incubated for 20 min at 37°C, followed by heating at 50°C for another 20 min and subsequently allowed to cool to room temperature. The turbidity of each reaction mixture was then measured spectrophotometrically at 660 nm wavelength to assess the extent of albumin denaturation inhibition by the AuNPs.

$$\text{Inhibition (\%)} = \frac{\text{Absorbance of Control} - \text{Absorbance of Sample}}{\text{Absorbance of Control}} \times 100$$

### Heat-induced hemolysis method

2 mL of human blood was obtained from a healthy volunteer and an erythrocyte suspension (10% v/v) was prepared using normal saline following established methods (Sakat *et al.*, 2010; Sadique *et al.*, 1989).

For the heat-induced hemolysis assay, varying amounts of AuNPs synthesized from seed and pod extracts of *E. cardamomum* were separately mixed with 3 mL of the erythrocyte suspension. The mixtures were then incubated at 55°C for 30 min to induce hemolysis. After incubation, the reaction mixtures were centrifuged for 10 min to separate the supernatant containing hemoglobin released from lysed erythrocytes. The optical density of the supernatant was measured at 560 nm using a spectrophotometer to quantify the extent of hemolysis.

## RESULTS

### Synthesis of AuNPs

AuNPs were successfully synthesized using aqueous extracts from seeds and pods of *E. cardamomum*. The extracts from both seed and pod appeared pale yellow prior to synthesis. Following the reaction, a distinct dark violet coloration was observed in both reaction mixtures, indicating the reduction of Au<sup>3+</sup> ions to Au nanoparticles. This color change serves as visual evidence of the effective bio-reduction capability of the seed and pod extracts, facilitating the formation of stable AuNPs through the reduction process. Thus, both extracts demonstrated their potential as efficient bio-reductants in the synthesis of gold nanoparticles Figure 1 (A) and (B).

### Characterization of AuNPs

#### UV-vis Spectra analysis

The UV spectra of AuNPs synthesized using aqueous extracts from *E. cardamomum* seed and pod are illustrated in Figure 2 (A) and (B) respectively. The spectrum of pod-mediated AuNPs exhibited a prominent peak at 545 nm, whereas the

## Synthesis of AuNPs

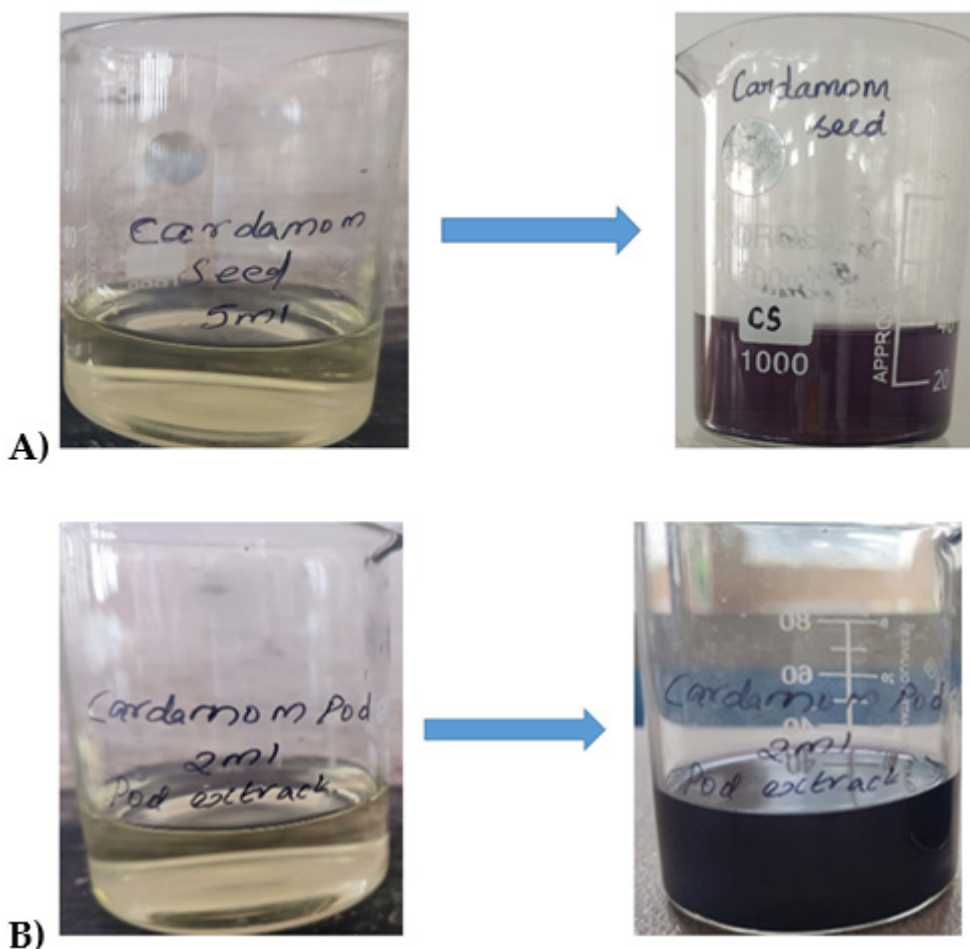


**Figure 1:** (A) *E. cardamomum* seed-mediated AuNPs. (B) *E. cardamomum* pod-mediated AuNPs.

## Characterization of AuNPs

### UV-vis Spectra analysis

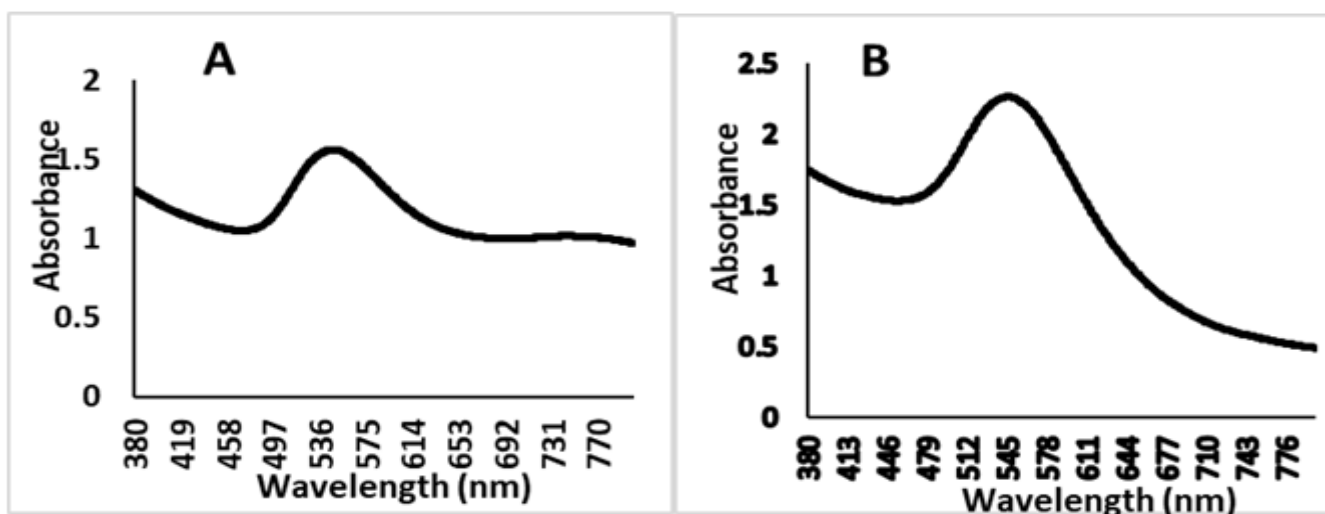


**Figure 2:** (A). UV-vis spectrum of *E. cardamomum* seed extract and its AuNPs. (B) UV-vis spectrum of *E. cardamomum* pod extract and its AuNPs.

seed-mediated AuNPs showed a strong absorption band centered around 550 nm. The Surface Plasmon Resonance (SPR) bands for nanoparticles mediated by seed and pod extracts were observed in the range of 530-565 nm, indicating the characteristic absorption of AuNPs. The broadening of these peaks in the UV spectra suggests the monodispersity of the synthesized nanoparticles. Notably, no significant color change or distinct absorption peaks were observed in the aqueous extracts of seed and pod alone, underscoring the role of *E. cardamomum* extracts in facilitating the synthesis and stabilization of gold nanoparticles with well-defined optical properties.

### X-ray (XRD) diffraction studies

Both samples from this study were subjected to XRD analysis using a Rigaku Miniflex 600 X-ray diffractometer. Cu K $\alpha$  radiation ( $\lambda=1.5406$  Å) was employed as the X-ray source and diffraction patterns were recorded at room temperature over a  $2\theta$  range of 10-80° with a step size of 0.02°. The XRD patterns for AuNPs synthesized using *E. cardamomum* seed and pod extracts are presented in Figure 3 (A) and (B), respectively, facilitating structural characterization. Both diffractograms exhibited prominent peaks indicative of the presence of AuNPs. Specifically, characteristic peaks for gold (Au) at (111), (200) and (220) were observed at  $2\theta$  values of 38.29°, 44.43° and 64.68°, confirming the crystalline nature of the synthesized nanoparticles. Additional unidentified peaks were also detected in the XRD patterns, suggesting potential minor crystalline phases or impurities in the synthesized AuNPs.

### Fourier Transform Infrared spectroscopy (FTIR) analysis

FTIR spectra of *E. cardamomum* seed extract, pod extract and their respective mediated AuNPs are presented in Figures 4 and 5, respectively. The FTIR spectrum of *E. cardamomum* seed extract revealed multiple absorption peaks at 1641.09, 3162.10, 3207.85,

3253.59, 3316.49, 3333.65, 3390.83, 3413.70, 3470.88 and 3522.34  $\text{cm}^{-1}$ . For seed-mediated AuNPs, characteristic IR absorption bands were observed at 1521.01, 1641.09, 3179.26, 3242.16, 3305.05, 3356.52, 3379.39, 3448.01 and 3522.34  $\text{cm}^{-1}$ . Similarly, the FTIR spectrum of *E. cardamomum* pod extract exhibited absorption bands at 1641.09, 3173.54, 3236.44, 3299.34, 3350.80, 3390.83, 3407.98, 3442.29 and 3505.19  $\text{cm}^{-1}$ , while pod-mediated AuNPs displayed peaks at 1641.09, 3179.26, 3219.28, 3236.44, 3305.05 and 3413.70  $\text{cm}^{-1}$ . The spectra of both extracts and their corresponding AuNPs exhibited similar patterns with slight variations in wavenumbers, indicative of successful synthesis and functionalization of AuNPs using seed and pod extracts. Key absorption peaks at 1641.09  $\text{cm}^{-1}$  corresponded to aromatic compounds (C-H bending), 3236.44  $\text{cm}^{-1}$  represented alcohol groups (O-H stretching) for pod extract and its AuNPs and peaks at 3407.98  $\text{cm}^{-1}$  and 3413.70  $\text{cm}^{-1}$  indicated amine groups (N-H stretching) for pod extract and pod-mediated AuNPs, respectively. Additionally, the vibrational band at 3522.34  $\text{cm}^{-1}$  for seed extract and its AuNPs corresponded to strong O-H bonds (alcohol), while peaks at 3333.65  $\text{cm}^{-1}$  and 3379.39  $\text{cm}^{-1}$  indicated amine groups (N-H stretching). These findings underscore the consistent biochemical features and functional groups involved in the synthesis and stabilization of AuNPs using *E. cardamomum* extracts.

### Scanning Electron Microscope (SEM) analysis

The morphology of AuNPs synthesized using extracts from seeds and pods of *E. cardamomum* was characterized using SEM. SEM images depicted in Figure 6 (A) and (B) illustrate the morphology of AuNPs synthesized from seed and pod extracts, respectively. The analysis revealed that the synthesized AuNPs exhibited an average size of approximately 20 nm and a spherical shape under room-temperature synthesis conditions. This uniformity in size and shape suggests efficient reduction and stabilization of AuNPs using *E. cardamomum* extracts.

### X-ray Diffraction Studies

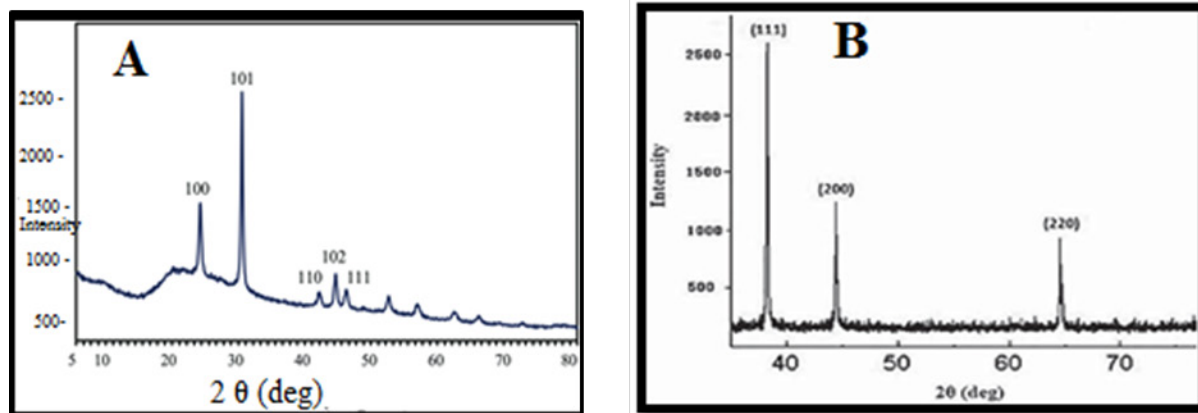


**Figure 3:** (A) XRD analysis for *E. cardamomum* seed-mediated synthesis of AuNPs; (B) XRD analysis for *E. cardamomum* pod-mediated synthesis of AuNPs.

### Energy-Dispersive X-ray (EDX) analysis

EDX was employed to analyze the elemental composition of Gold Nanoparticles (AuNPs) synthesized using *E. cardamomum* seed and pod extracts (Figure 7 (A) and (B)). The EDX spectra of both seed and pod-based AuNPs exhibited strong absorption band peaks at 2.2 keV, characteristic of gold absorption. This indicates the presence of elemental gold in the synthesized nanoparticles. Additionally, weak signals corresponding to other elements were observed in each spectrum of AuNPs, suggesting potential trace

elements or impurities present in the samples. The EDX results confirm the predominant composition of gold in both seed and pod-mediated AuNPs, corroborating their successful synthesis and purity using *E. cardamomum* extracts as reducing agents.

### Transmission Electron Microscopy (TEM) and Particle size analysis

TEM analysis was conducted on all samples to investigate the morphology and size distribution of the synthesized nanoparticles. As depicted in Figure 8, the majority of the

**Table 1: Anti-bacterial activity of pod mediated AuNPs.**

Test organism	Zone of inhibition (mm)				
	Pod-mediated AuNPs	Cefmetazole	Ampicillin	Tetracycline	Ciprofloxacin
<i>Escherichia coli</i>	12	-	-	-	-
<i>Klebsiella pneumoniae</i>	13	-	-	-	-
<i>Staphylococcus aureus</i>	10	-	-	-	-

### Fourier Transform Infrared (FTIR) analysis

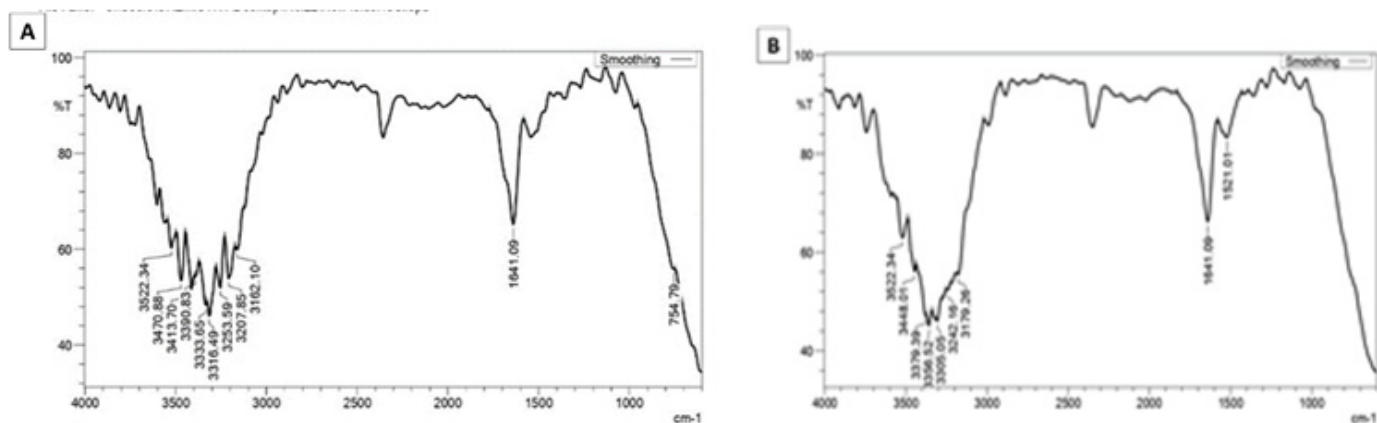


**Figure 4:** (A). FTIR analysis of *E. cardamomum* seed extract (B). FTIR analysis of *E. cardamomum* seed mediated AuNPs.

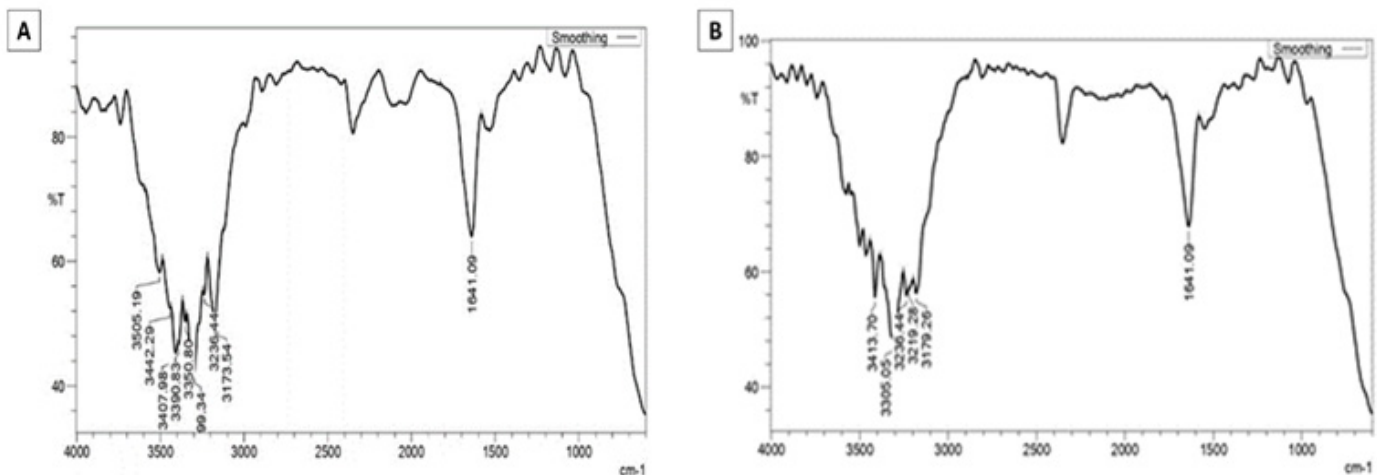


**Figure 5:** (A) FTIR analysis of *E. cardamomum* pod extract (B) FTIR analysis of *E. cardamomum* pod mediated AuNPs.

## SEM (Scanning Electron Microscope) analysis

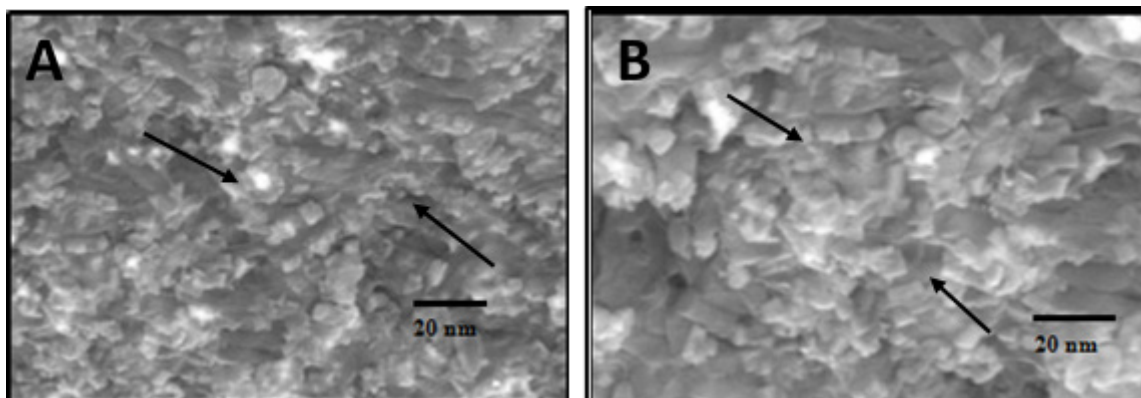


**Figure 6:** (A) SEM analysis of *E. cardamomum* seed-mediated synthesis of AuNPs; (B) SEM analysis of *E. cardamomum* pod-mediated synthesis of AuNPs.

## Energy-Dispersive X-Ray analysis

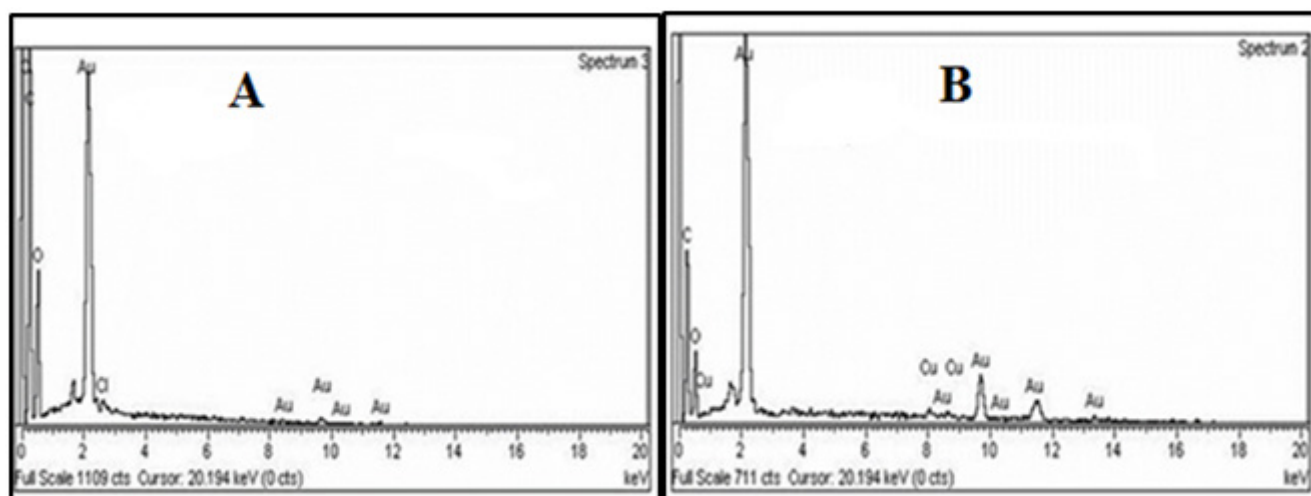


**Figure 7:** (A) EDX analysis of *E. cardamomum* seed-mediated synthesis of AuNPs; (B) EDX analysis of *E. cardamomum* pod-mediated synthesis of AuNPs.

## Transmission Electron Microscopy (TEM) and Particle size analysis

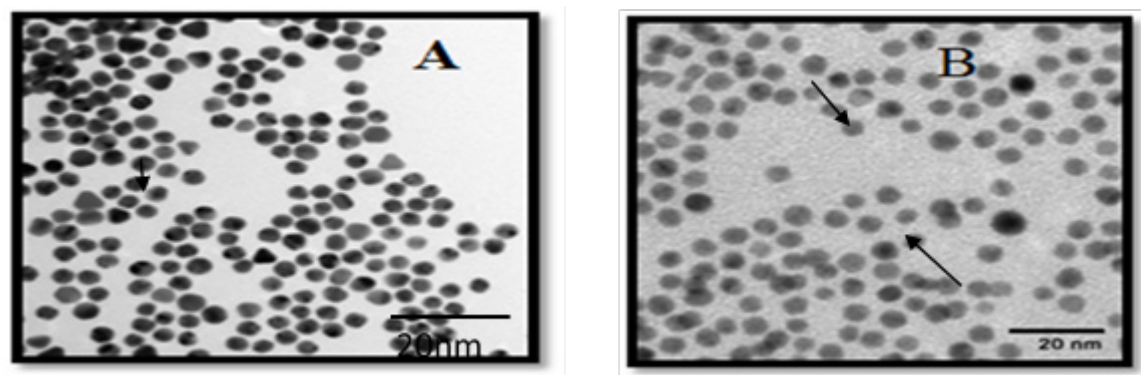


**Figure 8:** (A) TEM analysis of *E. cardamomum* seed-mediated synthesis of AuNPs; (B) TEM analysis of *E. cardamomum* pod-mediated synthesis of AuNPs.

samples exhibited geometric shapes with relatively low shape homogeneity, predominantly measuring around 20 nm in size. Figure 9 illustrates a broader size distribution, with particle sizes ranging from 5 nm to 65 nm. The median diameter, representing the average particle size, was estimated to be approximately 26 nm. These TEM findings provide detailed insights into the morphology and size characteristics of the synthesized nanoparticles using *E. cardamomum* extracts, highlighting both the uniformity and variability in particle sizes among the samples

### Antibacterial Activity

*E. cardamomum* pod-mediated AuNPs demonstrated potent bactericidal activity against the tested bacterial strains *Escherichia coli*, *Klebsiella pneumoniae* and *Staphylococcus aureus* (Figure 10). In contrast, AuNPs synthesized from *E. cardamomum* seeds did

not exhibit significant antibacterial effects against these organisms. The pod-mediated AuNPs showed the highest zone of inhibition against *Klebsiella pneumoniae*, measuring 13 mm, followed by 12 mm for *Staphylococcus aureus* and 10 mm for *Escherichia coli*. These findings highlight the effective antimicrobial potential of *E. cardamomum* pod-mediated AuNPs, suggesting their promising application in combating bacterial infections caused by these pathogenic strains.

AuNPs synthesized from *E. cardamomum* pods exhibited exceptional antibacterial efficacy compared to standard antibiotics such as cefmetazole, ampicillin, tetracycline and ciprofloxacin, all of which showed resistance against the tested bacterial strains. None of the antibiotics produced inhibitory zones against the bacterial strains tested. Among the bacterial strains evaluated, *Klebsiella pneumoniae* showed the highest susceptibility to *E.*

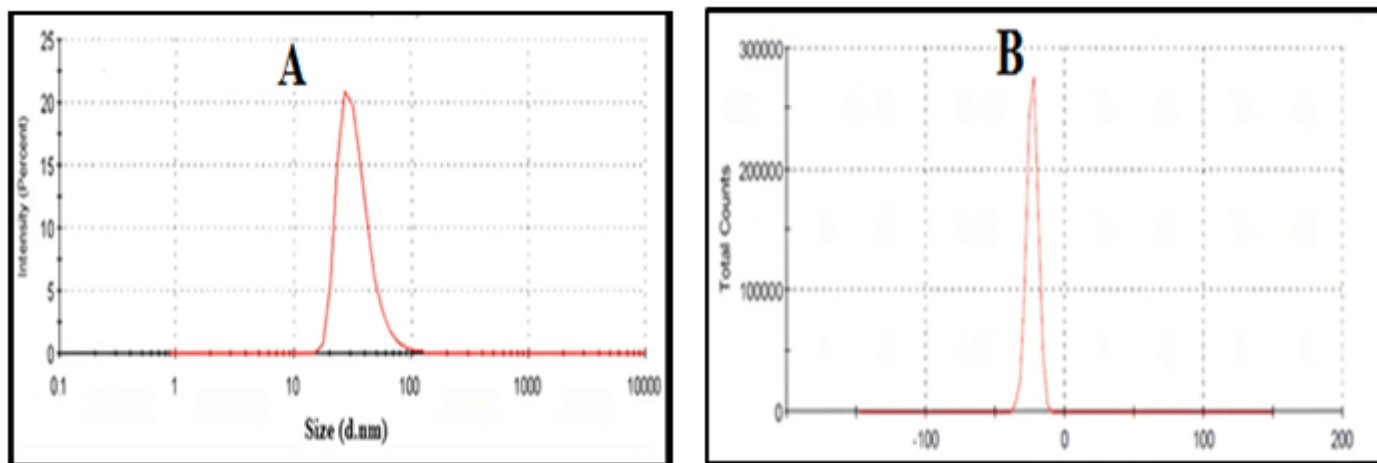


**Figure 9:** (A) Particle size analysis of *E. cardamomum* seed-mediated synthesis of AuNPs; (B) Particle size analysis of *E. cardamomum* pod-mediated synthesis of AuNPs.

### Antibacterial Activity

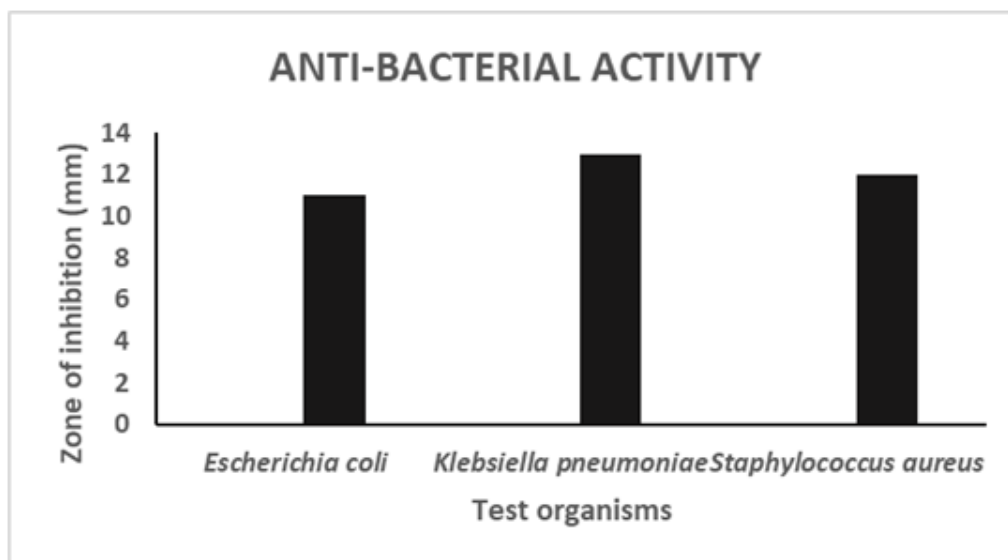


**Figure 10:** Anti-bacterial activity of synthesized AuNPs.

## Minimum Inhibitory Concentration (MIC)

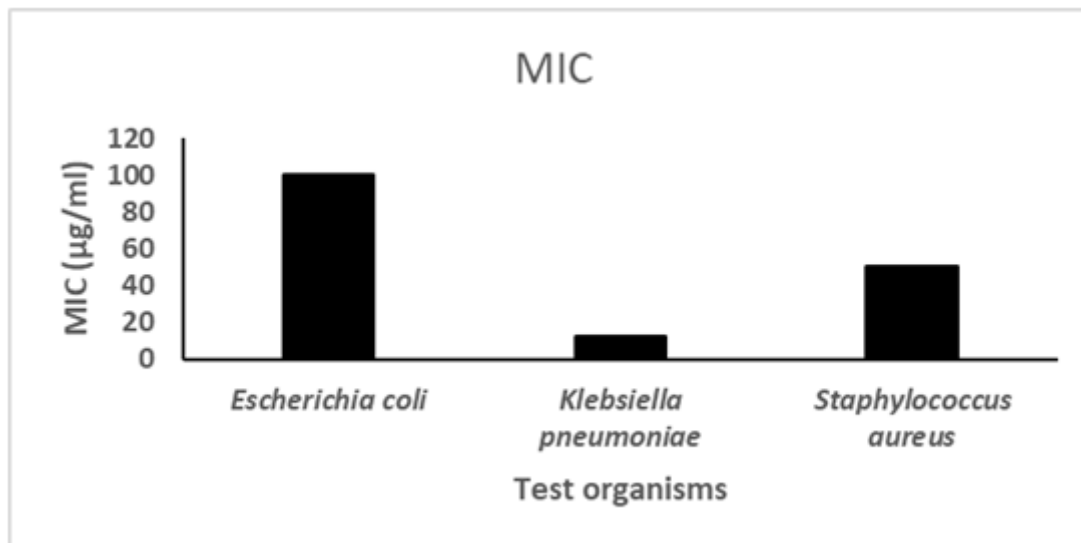


Figure 11: MIC of Pod-mediated AuNPs.

## Antioxidant Activity

### DPPH radical scavenging assay

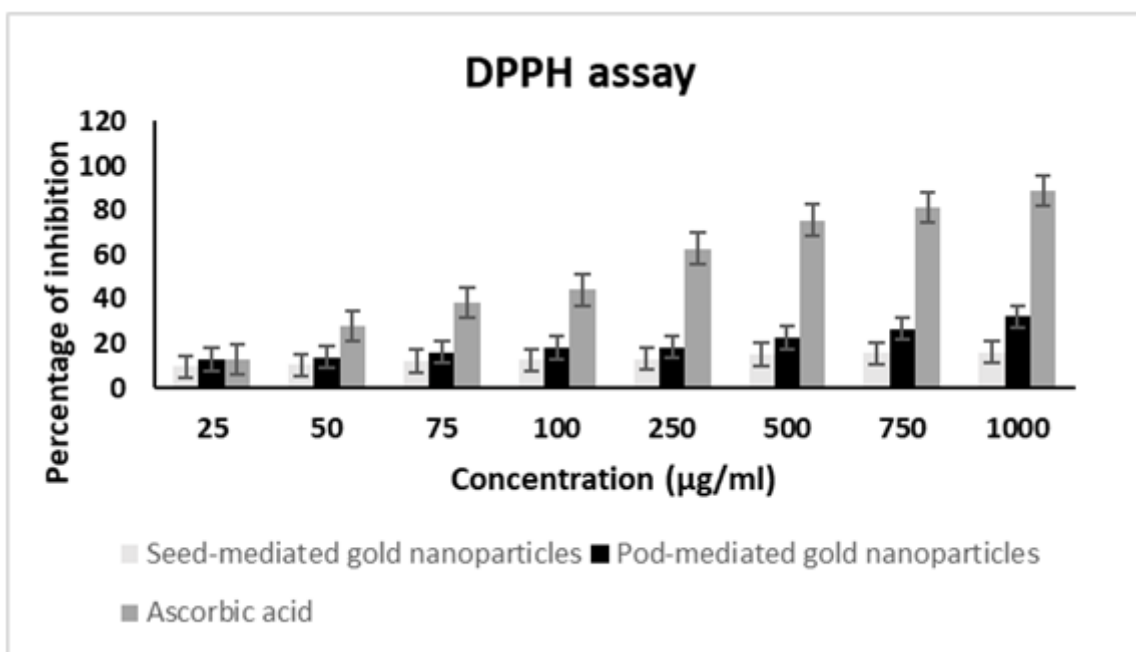


Figure 12: DPPH radical scavenging activity of synthesized AuNPs.

*cardamomum* pod-mediated AuNPs, with a maximum zone of inhibition measuring 13 mm. The detailed antibacterial activity of the synthesized AuNPs is summarized in Table 1.

## Minimum Inhibitory Concentration (MIC)

MIC values of *E. cardamomum* pod-mediated AuNPs are presented in Figure 11. Among the tested bacterial strains, *Klebsiella pneumoniae* exhibited the lowest MIC value of 12.5

µg/mL, indicating its highest susceptibility to *E. cardamomum* pod-mediated AuNPs. *Escherichia coli* showed a higher MIC value of 100 µg/mL, indicating greater resistance compared to *Staphylococcus aureus*, which had an MIC of 50 µg/mL. These MIC values underscore the differential susceptibility of bacterial strains to *E. cardamomum* pod-mediated AuNPs, highlighting their potential as effective antimicrobial agents against clinically relevant pathogens, particularly *Klebsiella pneumoniae*.

## Antioxidant Activity

### DPPH radical scavenging assay

The *E. cardamomum* seed and pod-mediated AuNPs exhibited concentration-dependent inhibition of DPPH radical (Figure 12). The maximum scavenging activity of pod-mediated nanoparticles was 31.94% at the concentration of 10 mg/mL, whereas for the seed-mediated nanoparticles, it was 15.87% at the

same concentration. The  $IC_{50}$  value for Pod and seed-mediated nanoparticles were 16.02 and 43.69 mg/mL, respectively. The lowest inhibition activity recorded was 9.55% and 12.67% at the concentration of 0.25 mg/mL of seed and pod-mediated AuNPs, respectively. The Pod-mediated AuNPs showed more significant DPPH radical scavenging activity than the seed-mediated nanoparticles.

### FRAP (Ferric Reducing Antioxidant Power) assay

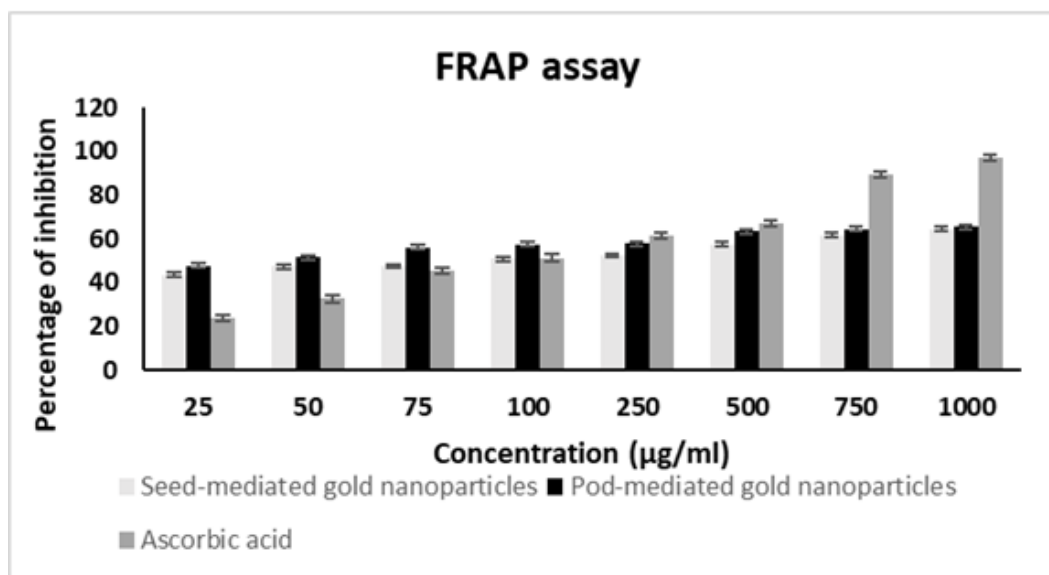


Figure 13: FRAP assay of synthesized AuNPs.

### Hydrogen peroxide scavenging activity

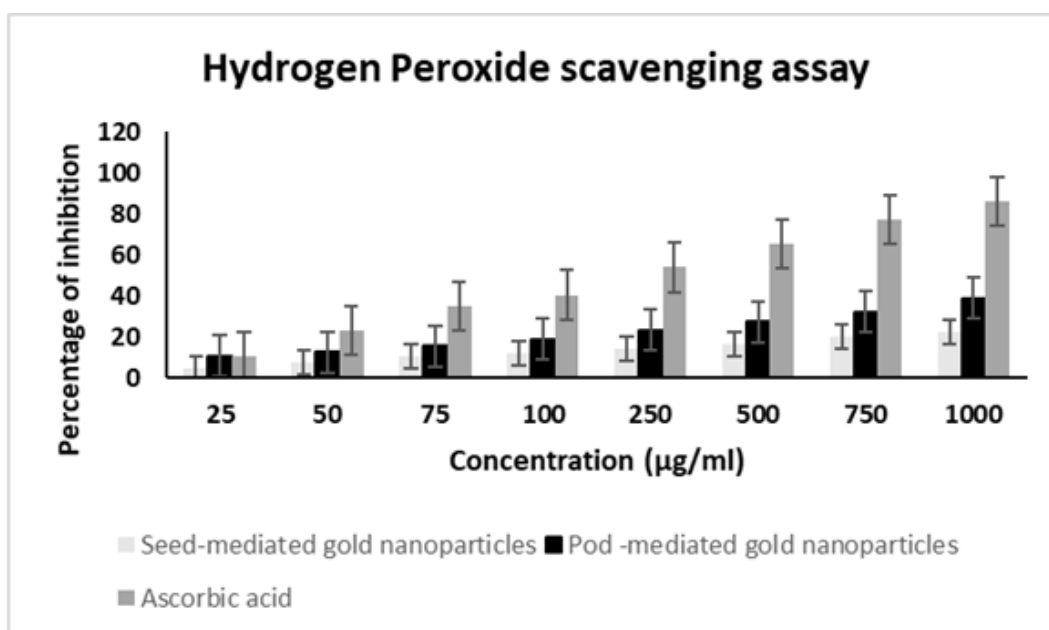


Figure 14: Hydrogen peroxide scavenging activity.

### FRAP (Ferric Reducing Antioxidant Power) assay

The data showed the maximum FRAP value of pod and seed-mediated nanoparticles were 65.62% and 64.55% respectively at the concentration of 1000  $\mu\text{g/mL}$  (Figure 13). The  $\text{IC}_{50}$  value was found to be 3.43  $\mu\text{g/mL}$  for seed-mediated AuNPs and 1.28  $\mu\text{g/mL}$  for pod-mediated AuNPs. The minimum inhibition was observed at the concentration of 25  $\mu\text{g/mL}$  of the seed-mediated AuNPs (43.6%) and pod-mediated AuNPs (47.85%) respectively. Hence, these findings indicated that the pod-mediated AuNPs possess higher FRAP activity than the seed-mediated AuNPs.

### Hydrogen peroxide scavenging activity

The data showed the maximum hydrogen peroxide scavenging value of Pod-mediated AuNPs was 38.72% and the  $\text{IC}_{50}$  value obtained was 11.42  $\mu\text{g/mL}$ . The Seed-mediated AuNPs exhibited the highest hydrogen scavenging activity of 22.39% and the  $\text{IC}_{50}$  was found to be 19.44  $\mu\text{g/mL}$ . The percentage of hydrogen peroxide scavenging activity of *E. cardamomum* seed and pod-mediated AuNPs was depicted in Figure 14. The hydrogen peroxide scavenging activity was observed to be increased with the increasing concentration of test samples such as seed and

### Reducing power assay

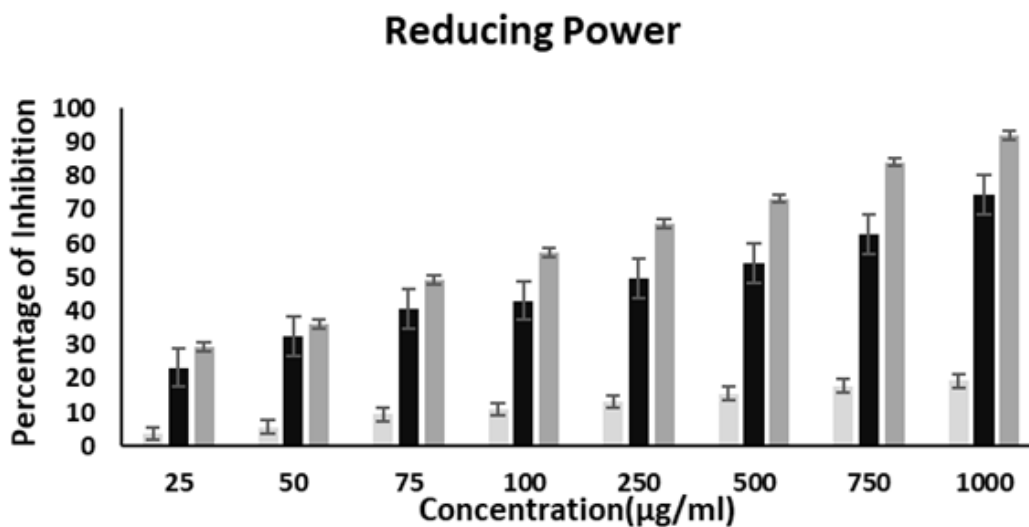


Figure 15: Reducing power assay of synthesized AuNPs.

### Phosphomolybdenum assay

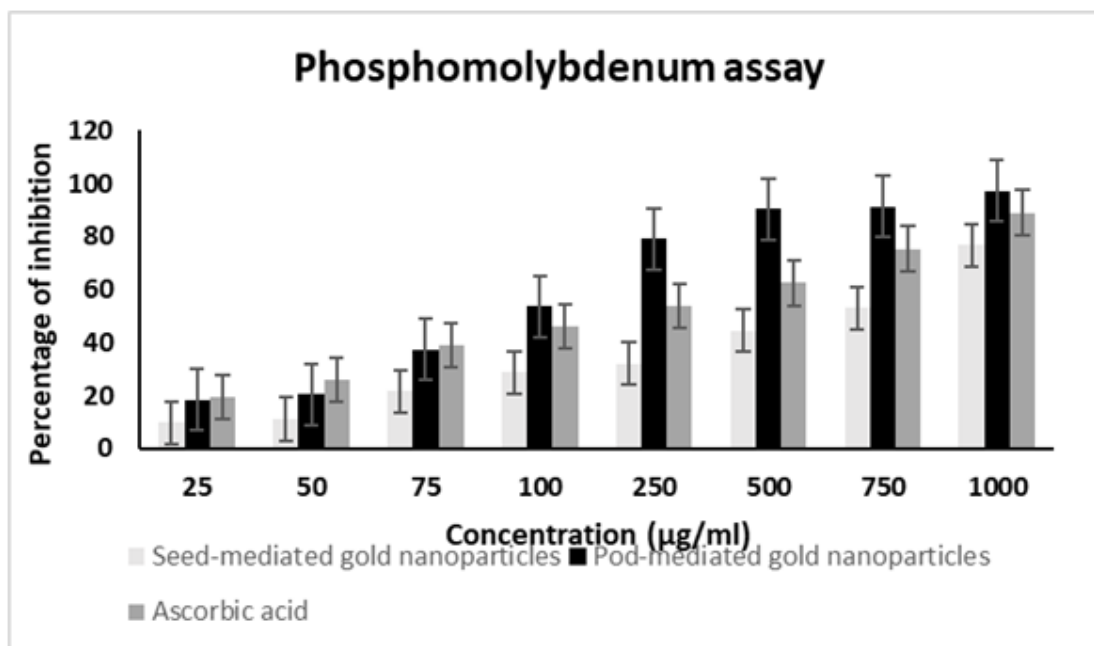


Figure 16: Phosphomolybdenum assay of synthesized AuNPs.

pod-synthesized AuNPs. The highest hydrogen scavenging activity was observed in the *E. cardamomum* pod-mediated AuNPs.

### Reducing power assay

The Reducing power assay showed the maximum inhibition value obtained for Pod-mediated AuNPs was 74.41% ( $IC_{50}$  = 4.86  $\mu$ g/mL), whereas the reducing activity was not found in the case of Seed-mediated AuNPs. The minimum percentage of

inhibition appeared to be 23.25% for the 25  $\mu$ g/mL concentration of *E. cardamomum* pod-mediated AuNPs. The results of *in vitro* antioxidant activity analyzed using a reducing power assay were presented in Figure 15.

### Phosphomolybdenum assay

The Phosphomolybdenum activity of AuNPs synthesized from the *E. cardamomum* seed and pod was increased with elevated concentration of the extracts (Figure 16). The maximum value of

### Anti-Inflammatory Activity

#### Albumin denaturation method

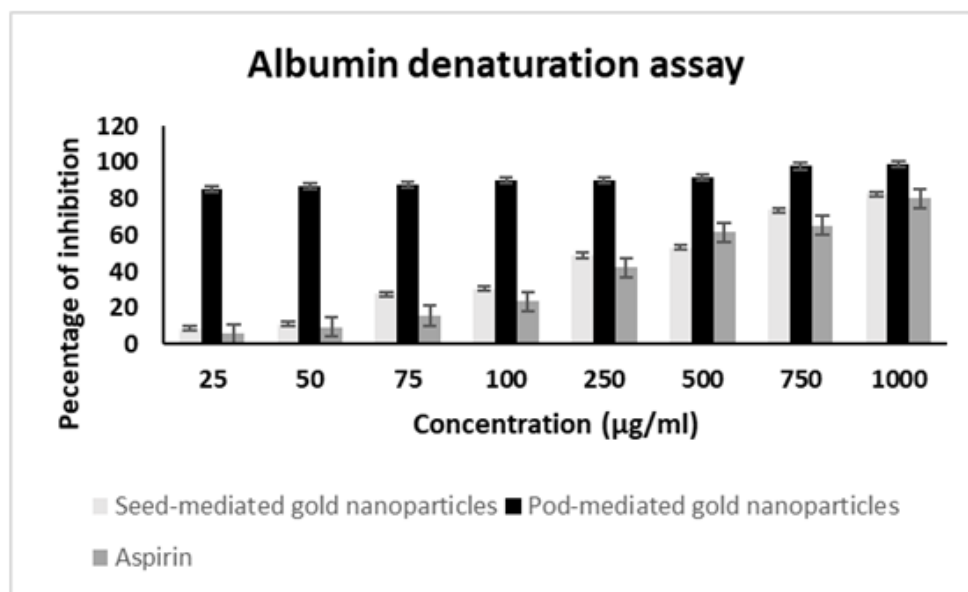


Figure 17: Albumin denaturation assay of synthesized AuNPs.

#### Heat-induced hemolysis method

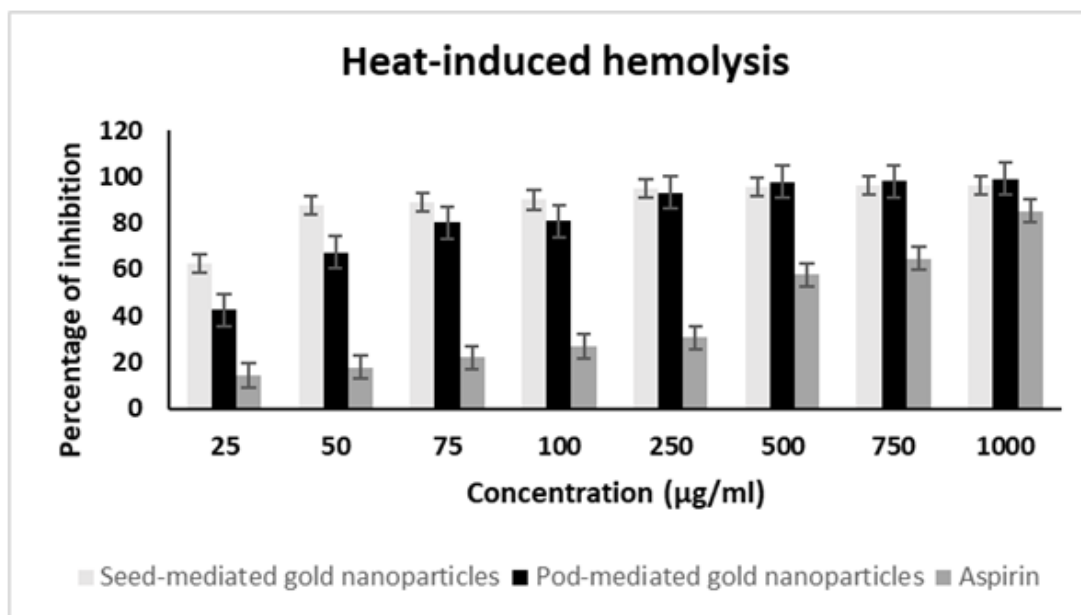


Figure 18: Heat-induced hemolysis of synthesized AuNPs.

pod-mediated nanoparticles was 97.05%, whereas 76.83% for the Seed-mediated nanoparticles at the concentration of 1000 µg/mL. The IC<sub>50</sub> value for Pod and Seed-mediated nanoparticles were 3.65 and 6.2 µg/mL, respectively. Hence, the highest percentage of phosphomolybdenum activity has occurred for the pod-mediated AuNPs than the Seed-mediated AuNPs.

## Anti-Inflammatory Activity

### Albumin denaturation method

In this current study, the *in vitro* anti-inflammatory activity of synthesized AuNPs was analyzed by the inhibitory activity against the denaturation of protein albumin (Figure 17). The *E. cardamomum* pod and Seed-mediated AuNPs inhibited the protein denaturation in a concentration-related manner. The highest inhibitory activity against albumin denaturation observed was 99.21% for pod-mediated AuNPs and 82.56% for Seed-mediated nanoparticles at the 1000 µg/mL concentration respectively. The IC<sub>50</sub> value calculated for the AuNPs synthesized from the seed and pod of *E. cardamomum* was 5.21 µg/mL and 1.29 µg/mL, respectively. The lowest percentage of inhibition against the denaturation of albumin was found to be 8.67% at 25 µg/mL concentration, whereas it was 85.43% for the pod-mediated AuNPs at the same concentration. Hence, these results clearly indicated that the *E. cardamomum* pod-mediated AuNPs have inhibited the albumin denaturation more effectively than the Seed-mediated AuNPs.

### Heat-induced hemolysis method

The *in vitro* anti-inflammatory potential of the AuNPs of *E. cardamomum* was determined by membrane stabilization of Red Blood Cells at various concentrations (Figure 18). All the tested concentrations of AuNPs synthesized from seed and pod of *E. cardamomum* respectively inhibited the heat-induced hemolysis and these results contributed additional evidence for their anti-inflammatory effect. The maximum percentage inhibition was recorded as 96.53% (IC<sub>50</sub>=5.61 µg/mL) and 99.21% (IC<sub>50</sub>=5.16 µg/mL) for seed and pod-mediated AuNPs. The results demonstrated that Pod-mediated AuNPs exhibited effective membrane stabilizing activity by preventing the lysis of erythrocytes induced by heat than the seed-mediated AuNPs.

## DISCUSSION

Spices and aromatic plants have long played a crucial role in traditional medicine across various cultures. Spices serve not only as flavor enhancers, colorants and preservatives but also as home remedies for a range of ailments (Viuda-Martos *et al.*, 2010). *E. cardamomum* is renowned for its pharmacological properties, including cytotoxic, antibacterial, anti-oncogenic and antioxidant effects (Ashokkumar *et al.*, 2020). In this study, AuNPs were successfully synthesized using an aqueous extract of *E. cardamomum* seeds and pods as reducing agents. The

formation of AuNPs was evidenced by a color change from pale yellow to dark violet. To our knowledge, this study represents the first attempt to compare the antibacterial, antioxidant and anti-inflammatory properties of AuNPs synthesized from *E. cardamomum* seeds and pods.

The AuNPs synthesized from different concentrations of *E. cardamomum* extracts, such as 1:1 and 1:10, exhibited characteristic absorption peaks at 530 nm and 550 nm, respectively. Previous studies have reported similar findings, noting a surface Plasmon resonance (Pattanayak and Nayak, 2013). (SPR) band at 527 nm for AuNPs synthesized using aqueous extracts of *E. cardamomum* seeds (Rajan *et al.*, 2017), and a sharp peak at 526 nm for those synthesized with black cardamom extract (Singh and Srivastava, 2015). Shah *et al.*, 2022, demonstrated an absorption peak at 535 nm for AuNPs synthesized using *Sageretia thea* leaves, with absorption intensity increasing proportionally with AuNP concentration in the reaction mixture.

The X-ray Diffraction (XRD) studies of AuNPs of aqueous extract prepared using *Amomum villosum* and *E. cardamomum* exhibited four distant diffraction peaks at (111), (200), (220) and (311) with  $2\theta$  values of 38.49°, 44.44°, 65.07° and 77.82° respectively (Soshnikova *et al.*, 2018). However, the characteristic intense peaks at  $2\theta$ =(111) 38.47°, (200) 44.53°, (220) 64.80°, (311) 77.86° and (222) 82.65° was reported for the green synthesized AuNPs of *E. cardamomum* seeds by Rajan *et al.*, 2017. Moreover, the previous study carried out by Chen *et al.*, 2019, showed that the XRD peaks were located at  $2\theta$ =38.179° (111), 44.375° (200), 64.50° (220), 77.546° (311) and 81.700° (222) for the green synthesized AuNPs of *Chenopodium formosanum* shell recorded using Cu K $\alpha$  radiation ( $\lambda$ =1.54184 Å).

The FTIR analysis of *Annona muricata* leaf extract showed the IR absorption bands at 1635.99, 2114.93 and 3284.47 cm<sup>-1</sup> whereas, the 1637.82, 2111.91 and 3271.14 cm<sup>-1</sup> for AuNPs synthesized leaf extract of *Annona muricata* (Folorunso *et al.*, 2019). The *E. cardamomum* seed extract yields strong bands at 1689, 1632, 1536, 1360, 1159, 1024 and 730 cm<sup>-1</sup>. A minor shift in wave numbers may be seen in the spectrum of AuNPs with a relatively identical peak (Rajan *et al.*, 2017), which was compromised with our results. Due to the presence of NH or OH groups in the extract, Au<sup>+3</sup> ions were converted to Au metal. The change in the peak of the carboxylic ketonic group from 1,728 to 1,635 cm<sup>-1</sup> may be an indication of the formation of AuNPs (Bawazeer *et al.*, 2022). Likewise, the findings of Soshnikova *et al.*, 2018, demonstrated that the primary -OH alcohol, C=C, aliphatic -CH and alcohol C-O groups, which are responsible for the vibrational bands at 3375.45, 2928.54, 1608.89 and 1022.17 cm<sup>-1</sup> in the FTIR spectra of dried fruits of *Amomum villosum* and synthesized AuNPs.

SEM analysis of Gold Nanoparticles (AuNPs) synthesized from *Garcinia kola* (ripe fruit) revealed the presence of spherical-shaped particles (Akintelu *et al.*, 2021). Similarly, SEM

images of AuNPs synthesized from *Ziziphus zizyphus* leaf extract exhibited spherical and poly-crystalline particles (Aljabali *et al.*, 2018) Rajan *et al.*, 2017, reported the synthesis of 100 nm-sized AuNPs from *E. cardamomum* seeds, a finding consistent with the current study, which also observed spherical-shaped AuNPs of approximately 100 nm in size through SEM examination.

Bawazeer *et al.*, 2022, found strong signals for Gold (Au) atoms at 0.4 and 2.7 keV in the EDX profile of black pepper-synthesized AuNPs, with weaker signals at 6.2, 9.8 and 11.6 keV. Similarly, Alhumaydhi *et al.*, 2021, observed strong signals at 0.5 and 2.3 keV, with a weak signal at 9.8 keV in saffron-based nanoparticles. Bahattab *et al.*, 2021, also confirmed the formation of AuNPs from black cumin seeds using EDX analysis, noting substantial signals at approximately 2 keV and weaker signals at 9.7, 10.2 and 11.7 keV.

Transmission Electron Microscopy (TEM) analysis by Rajan *et al.*, 2017, showed 100 nm-sized AuNPs synthesized from *E. cardamomum* seeds. Salari *et al.*, 2019, reported the synthesis of spherical-shaped AuNPs ranging from 2 to 10 nm using aerial parts of *Cuminum cyminum*. Particle size analysis of *E. cardamomum* AuNPs revealed nanoparticles with diameters averaging 432.3 nm (Pattanayak and Nayak, 2013). Sunderam *et al.*, 2019, found an average size of 40 nm for AuNPs synthesized from *Anacardium occidentale* leaves.

Regarding antibacterial activity, Rajan *et al.*, 2017, reported moderate effects of *E. cardamomum* seed-synthesized AuNPs against *Staphylococcus aureus*, *Escherichia coli* and *Pseudomonas aeruginosa*, contrasting our results. Omprakash and Sharada, 2015, found considerable bactericidal activity of silver nanoparticles from *E. cardamomum* seeds against *Bacillus subtilis* and *Klebsiella planticola*. Moulai-Hacene *et al.*, 2020, reported an MIC of 6.25 mg/mL<sup>-1</sup> for *E. cardamomum* seed extract against *Carnobacterium maltoaromaticum*, *Bacillus cereus* and *Enterobacter* sp. Poyil and Shamna, 2022, found MIC values of 7.8 mg for multi-drug resistant *Klebsiella pneumoniae* and 3.9 mg for *Staphylococcus aureus* using methanolic *E. cardamomum* pod extract.

In this study, AuNPs synthesized from *E. cardamomum* seeds and pods exhibited dose-dependent *in vitro* antioxidant activity, with pod-mediated AuNPs demonstrating significant antioxidant potential. Similar concentration-related DPPH radical scavenging activity was reported for Cardamom fruits (Soshnikova *et al.*, 2018). Prakash *et al.*, 2012, found IC<sub>50</sub> values of 8.25±2.0 and 21.6±2.0 for ethanolic and aqueous extracts of large cardamom (*Amomum subulatum*), respectively, in the DPPH assay. Bhatti *et al.*, 2010, reported an IC<sub>50</sub> value of 17.26 µg/mL for methanolic *E. cardamomum* (70%) in the DPPH assay. Singh *et al.*, 2008, recorded potent antioxidant activity for essential oils and oleoresins from *E. cardamomum* seeds and pods, supporting

our findings. Arista *et al.*, 2023, highlighted the antioxidant potential of Cardamom (*Amomum compactum*) fruits, enriched with bioactive compounds. Tahir *et al.*, 2015, found effective inhibition of free radicals by AuNPs synthesized from *Nerium oleander* leaves, comparable to our results.

Furthermore, this study demonstrated that *E. cardamomum* pod-synthesized AuNPs exhibited more pronounced *in vitro* anti-inflammatory effects compared to seed-synthesized AuNPs. Souissi *et al.*, 2020, reported similar effects using seed extract. Arpitha *et al.*, 2019, found significant reduction in inflammation with *E. cardamomum* seed oil and resin in a carrageenan-induced paw edema model. Kandikattu *et al.*, 2017, observed reduced paw inflammation with intraperitoneal hexane extract of *Elettaria repens* (big cardamom) in the same model. This study highlights the multifaceted potential of *E. cardamomum* nanoparticles in combating microbial infections, oxidative stress and inflammatory conditions. The environmentally friendly synthesis process underscores the sustainable approach of utilizing natural resources for nanoparticle production.

## CONCLUSION

In conclusion, AuNPs synthesized using the aqueous extracts of *E. cardamomum* seed and pod, characterized by their spherical morphology and average size of 20 nm. The AuNPs synthesized from *E. cardamomum* pods exhibited notable antioxidant properties, as evidenced by their performance in various assays including DPPH, FRAP, hydrogen peroxide scavenging, reducing power and phosphomolybdenum assay. Additionally, these nanoparticles demonstrated significant anti-inflammatory effects by effectively inhibiting albumin denaturation and heat-induced hemolysis. While exhibiting moderate antibacterial activity against tested strains, the pod-mediated nanoparticles showed superior antioxidant, antibacterial and anti-inflammatory properties compared to those synthesized from seeds.

This comparative analysis underscores the potential of *E. cardamomum* pods as a promising natural source for synthesizing AuNPs with robust pharmacological effects. The cost-effectiveness and widespread availability of *E. cardamomum* pods further enhance their suitability for large-scale nanoparticle production. Overall, this research contributes valuable insights into the medicinal applications of plant-mediated nanoparticles, highlighting the significance of exploring natural resources for synthesizing nanomaterials with therapeutic potentials.

## ACKNOWLEDGEMENT

The authors are grateful to the management as well as the faculty members in the, Department of Biochemistry, Kongunadu Arts and Science College (Autonomous), G.N. Mills P.O, Coimbatore-641029, Tamil Nadu, India for providing the support to fulfil this work.

## CONFLICT OF INTEREST

The authors declare that they have no known competing financial interests or personal relationships that could have appeared to influence the work reported in this paper.

## REFERENCES

- Akintelu, S. A., Yao, B., & Folorunso, A. S. (2021). Green synthesis, characterization and antibacterial investigation of synthesized gold nanoparticles (AuNPs) from *Garcinia kola* pulp extract. *Plasmonics*, 16(1), 157–165. <https://doi.org/10.1007/s11468-020-01274-9>
- Alhumaydhi, F. A., Khan, I., Rauf, A., Qureshi, M. N., Aljohani, A. S. M., Khan, S. A., Khalil, A. A., El-Esawi, M. A., & Muhammad, N. (2021). Synthesis, characterization, biological activities and catalytic applications of alcoholic extract of saffron (*Crocus sativus*) flower stigma-based gold nanoparticles. *Green Processing and Synthesis*, 10(1), 230–245. <https://doi.org/10.1515/gps-2021-0024>
- Aljabali, A. A., Akkam, Y., Al Zoubi, M. S., Al-Batayneh, K. M., Al-Trad, B., Abo Alrob, O., Alkilany, A. M., Benamara, M., & Evans, D. J. (2018). Synthesis of gold nanoparticles using leaf extract of *Ziziphus zizyphus* and their antimicrobial activity. *Nanomaterials*, 8(3), 174. <https://doi.org/10.3390/nano8030174>
- Arista, R. A., Priosoeryanto, B. P., & Nurcholis, W. (2023). Profile volatile compounds in essential oils on different parts of cardamom with antioxidant activity. *Biointerface res. Journal of Applied Chemistry*, 13(4), 328. <https://doi.org/10.33263/BRIAC134.328>
- Arpitha, S., Srinivasan, K., & Sowbhagya, H. B. (2019). Anti-inflammatory effect of resin fraction of cardamom (*E. cardamomum*) in carrageenan-induced rat paw edema. *PharmaNutrition*, 10, Article 100165. <https://doi.org/10.1016/j.phanu.2019.100165>
- Ashokkumar, K., Murugan, M., Dhanya, M. K., & Warkentin, T. D. (2020). Botany, traditional uses, phytochemistry and biological activities of cardamom [*E. cardamomum* (L.) Maton]-A critical review. *Journal of Ethnopharmacology*, 246, Article 112244. <https://doi.org/10.1016/j.jep.2019.112244>
- Bahattab, O., Khan, I., Bawazeer, S., Rauf, A., Qureshi, M. N., Al-Awthan, Y. S., Muhammad, N., Khan, A., Akram, M., Islam, M. N., & Bin Emran, T. (2021). Synthesis and biological activities of alcohol extract of black cumin seeds (*Bunium persicum*)-based gold nanoparticles and their catalytic applications. *Green Processing and Synthesis*, 10(1), 440–455. <https://doi.org/10.1515/gps-2021-0041>
- Bano, S., Ahmad, N., & Sharma, A. K. (2016). Phytochemical screening and evaluation of anti-microbial and anti-oxidant activity of *Elettaria cardamom* (Cardamom). *Journal of Applied and Natural Science*, 8(4), 1966–1970. <https://doi.org/10.31018/jans.v8i4.1071>
- Bawazeer, S., Khan, I., Rauf, A., Aljohani, A. S. M., Alhumaydhi, F. A., Khalil, A. A., Qureshi, M. N., Ahmad, L., & Khan, S. A. (2022). Black pepper (*Piper nigrum*) fruit-based gold nanoparticles (BP-AuNPs): Synthesis, characterization, biological activities and catalytic applications-A green approach. *Green Processing and Synthesis*, 11(1), 11–28. <https://doi.org/10.1515/gps-2022-0002>
- Bhatti, H. N., Zafar, F., & Jamal, M. A. (2010). Evaluation of phenolic contents and antioxidant potential of methanolic extracts of green cardamom (*E. cardamomum*). *Asian Journal of Chemistry*, 22(6), 4787.
- Boggula, N., Reddy, S. R., Alla, T. S., Farhana, A., Battineni, J., & Bakshi, V. (2017). Phytochemical evaluation and in vitro antibacterial activity of dried seeds of *Abrus precatorius*. *International Journal of Pharmaceutical Sciences Review and Research*, 44(1), 101–107.
- Chen, M.-N., Chan, C.-F., Huang, S.-L., & Lin, Y.-S. (2019). Green biosynthesis of gold nanoparticles using *Chenopodium formosanum* shell extract and analysis of the particles' antibacterial properties. *Journal of the Science of Food and Agriculture*, 99(7), 3693–3702. <https://doi.org/10.1002/jsfa.9600>
- Dikshit, P. K., Kumar, J., Das, A. K., Sadhu, S., Sharma, S., Singh, S., Gupta, P., & Kim, B. (2021). Green synthesis of metallic nanoparticles: Applications and limitations. *Catalysts*, 11(8), 902. <https://doi.org/10.3390/catal11080902>
- Elshikh, M., Ahmed, S., Funston, S., Dunlop, P., McGaw, M., Marchant, R., & Banat, I. M. (2016). Resazurin-based 96-well plate microdilution method for the determination of minimum inhibitory concentration of biosurfactants. *Biotechnology Letters*, 38(6), 1015–1019. <https://doi.org/10.1007/s10529-016-2079-2>
- Folorunso, A., Akintelu, S., Oyebamiji, A. K., Ajayi, S., Abiola, B., Abdusalam, I., & Morakinyo, A. (2019). Biosynthesis, characterization and antimicrobial activity of gold nanoparticles from leaf extracts of *Annona muricata*. *Journal of Nanostructure in Chemistry*, 9(2), 111–117. <https://doi.org/10.1007/s40097-019-0301-1>
- Govindappa, M., Hemashekar, B., Arthikala, M.-K., Ravishankar Rai, V. R., & Ramachandra, Y. L. (2018). Characterization, antibacterial, antioxidant, antidiabetic, anti-inflammatory and antityrosinase activity of green synthesized silver nanoparticles using *Calophyllum tomentosum* leaves extract. *Results in Physics*, 9, 400–408. <https://doi.org/10.1016/j.rinp.2018.02.049>
- Guo, C., Yang, J., Wei, J., Li, Y., Xu, J., & Jiang, Y. (2003). Antioxidant activities of peel, pulp and seed fractions of common fruits as determined by FRAP assay. *Nutrition Research*, 23(12), 1719–1726. <https://doi.org/10.1016/j.nutres.2003.08.005>
- Herizchi, R., Abbasi, E., Milani, M., & Akbarzadeh, A. (2016). Current methods for synthesis of gold nanoparticles. *Artificial Cells, Nanomedicine, and Biotechnology*, 44(2), 596–602. <https://doi.org/10.3109/21691401.2014.971807>
- Kandikattu, H. K., Rachitha, P., Jayashree, G. V., Krupashree, K., Sukhith, M., Majid, A., Amruta, N., & Khanum, F. (2017). Anti-inflammatory and anti-oxidant effects of Cardamom (*Elettaria repens* (Sonn.) Baill) and its phytochemical analysis by 4D GCXGC TOF-MS. *Biomedicine and Pharmacotherapy*, 91, 191–201. <https://doi.org/10.1016/j.biopha.2017.04.049>
- Kumar, J. A., Krithiga, T., Manigandan, S., Sathish, S., Renita, A. A., Prakash, P., Prasad, B. S. N., Kumar, T. R. P., Rajasimman, M., Hosseini-Bandegharai, A., Prabhu, D., & Crispin, S. (2021). A focus to green synthesis of metal/metal based oxide nanoparticles: Various mechanisms and applications towards ecological approach. *Journal of Cleaner Production*, 324, Article 129198. <https://doi.org/10.1016/j.jclepro.2021.129198>
- Modena, M. M., Rühle, B., Burg, T. P., & Wuttke, S. (2019). Nanoparticle characterization: What to measure? *Advanced Materials*, 31(32), Article e1901556. <https://doi.org/10.1002/adma.201901556>
- Moulai-Hacene, F., Boufadi, M. Y., Keddari, S., & Homrani, A. (2020). Chemical composition and antimicrobial properties of *E. cardamomum* extract. *Pharmacognosy Journal*, 12(5), 1058–1063. <https://doi.org/10.5530/pj.2020.12.149>
- Muniyappan, N., Pandeewaran, M., & Amalraj, A. (2021). Green synthesis of gold nanoparticles using *Curcuma pseudomontana* isolated curcumin: Its characterization, antimicrobial, antioxidant and anti-inflammatory activities. *Environmental Chemistry and Ecotoxicology*, 3, 117–124. <https://doi.org/10.1016/j.encco.2021.01.002>
- Omprakash, V., & Sharada, S. (2015). Green synthesis and characterization of silver nanoparticles and evaluation of their antibacterial activity using *Elettaria cardamom* seeds. *Journal of Nanomedicine and Nanotechnology*, 6(2). <https://doi.org/10.4172/2157-7439.1000266>
- Patil, S., & Chandrasekaran, R. (2020). Biogenic nanoparticles: A comprehensive perspective in synthesis, characterization, application and its challenges. *Journal, Genetic Engineering & Biotechnology*, 18(1), 67. <https://doi.org/10.1186/s43141-020-00081-3>
- Pattanayak, M., & Nayak, P. L. (2013). Green synthesis of AuNPs using *E. cardamomum* (ELAICHI) aqueous extract. *World*, 2, 1–5.
- Poyil, M. M., & Shamna, K. P. (2022). Antibacterial Potential of Methanolic Extract of Cardamom (*E. cardamomum*) Pods against Multidrug Resistant *Klebsiella pneumoniae* and *Staphylococcus aureus*. *Applied Biological Research*, 24(2), 203–209. <https://doi.org/10.5958/0974-4517.2022.00024.6>
- Prakash, K. D., Brajesh, K., Arshad, H., Shikhar, V., & Mala, M. (2012). Evaluation of antioxidant activity of large cardamom (leaves of *Amomum subulatum*). *International Journal of Drug Development and Research*, 4(1), 175–179.
- Rajan, A., Rajan, A. R., & Philip, D. (2017). *E. cardamomum*. *OpenNano*, 2, 1–8. <https://doi.org/10.1016/j.onano.2016.11.002>
- Sadique, J., Al-Rqobah, W. A., Bughaith, M. F., & El-Gindy, A. R. The bio-activity of certain medicinal plants on the stabilization of RBC membrane system. *Fitoterapia*, 60, 525–532.
- Sahreen, S., Khan, M. R., & Khan, R. A. (2010). Evaluation of antioxidant activities of various solvent extracts of *Carissa opaca* fruits. *Food Chemistry*, 122(4), 1205–1211. <https://doi.org/10.1016/j.foodchem.2010.03.120>
- Sahu, M. K., Yadav, R., & Tiwari, S. P. (2023). Recent advances in nanotechnology. *International Journal of Nanomaterials, Nanotechnology and Nanomedicine*, 9(1), 015–023. <https://doi.org/10.17352/2455-3492.000053>
- Sakat, S., Juvekar, A. R., & Gambhire, M. N. (2010). In vitro antioxidant and anti-inflammatory activity of methanol extract of *Oxalis corniculata* Linn. *International Journal of Pharmacy and Pharmaceutical Sciences*, 2(1), 146–155.
- Salari, N., Karimi Maleh, H., & Asadi, M. (2019). Biosynthesis of gold nanoparticles by extract of aerial organs of Cumin (*Cuminum cyminum* L.). *Cellular and molecular research (Iranian journal of biology)*, 32(3), 286–296. <https://doi.org/10.1007/s00011-019-00011-1>
- Saratale, R. G., Saratale, G. D., Shin, H. S., Jacob, J. M., Pugazhendhi, A., Bhaishare, M., & Kumar, G. (2018). New insights on the green synthesis of metallic nanoparticles using plant and waste biomaterials: Current knowledge, their agricultural and environmental applications. *Environmental Science and Pollution Research International*, 25(11), 10164–10183. <https://doi.org/10.1007/s11356-017-9912-6>
- Sarker, S. D., Nahar, L., & Kumarasamy, Y. (2007). Microtitre plate-based antibacterial assay incorporating resazurin as an indicator of cell growth and its application in the in vitro antibacterial screening of phytochemicals. *Methods*, 42(4), 321–324. <https://doi.org/10.1016/j.jymeth.2007.01.006>
- Shah, S., Shah, S. A., Faisal, S., Khan, A., Ullah, R., Ali, N., & Bilal, M. (2022). Engineering novel gold nanoparticles using *Sageretia thea* leaf extract and evaluation of their biological activities. *Journal of Nanostructure in Chemistry*, 12(1), 129–140. <https://doi.org/10.1007/s40097-021-00407-8>
- Shimada, K., Fujikawa, K., Yahara, K., & Nakamura, T. (1992). Antioxidative properties of xanthan on the autoxidation of soybean oil in cyclodextrin emulsion. *Journal of Agricultural and Food Chemistry*, 40(6), 945–948. <https://doi.org/10.1021/jf00018a005>
- Singh, A. K., & Srivastava, O. N. (2015). One-step green synthesis of gold nanoparticles using black cardamom and effect of pH on its synthesis. *Nanoscale Research Letters*, 10(1), 1055. <https://doi.org/10.1186/s11671-015-1055-4>
- Singh, G., Kiran, S., Marimuthu, P., Isidorov, V., & Vinogorova, V. (2008). Antioxidant and antimicrobial activities of essential oil and various oleoresins of *E. cardamomum* (seeds and pods). *Journal of the Science of Food and Agriculture*, 88(2), 280–289. <https://doi.org/10.1002/jsfa.3087>

- SivaKumar, T., Rathimeena, T., Thangapandian, V., & Shankar, T. (2015). Silver nanoparticles synthesis of *Mentha arvensis* extracts and evaluation of antioxidant properties. *Journal of Bioscience and Bioengineering*, 1, 22–28.
- Soshnikova, V., Kim, Y. J., Singh, P., Huo, Y., Markus, J., Ahn, S., Castro-Aceituno, V., Kang, J., Chokkalingam, M., Mathiyalagan, R., & Yang, D. C. (2018). Cardamom fruits as a green resource for facile synthesis of gold and silver nanoparticles and their biological applications. *Artificial Cells, Nanomedicine, and Biotechnology*, 46(1), 108–117. <https://doi.org/10.1080/21691401.2017.1296849>
- Souissi, M., Azelmat, J., Chaieb, K., & Grenier, D. (2020). Antibacterial and anti-inflammatory activities of cardamom (*E. cardamomum*) extracts: Potential therapeutic benefits for periodontal infections. *Anaerobe*, 61, Article 102089. <https://doi.org/10.1016/j.anaerobe.2019.102089>
- Sunderam, V., Thiyagarajan, D., Lawrence, A. V., Mohammed, S. S. S., & Selvaraj, A. (2019). In vitro antimicrobial and anticancer properties of green synthesized gold nanoparticles using *Anacardium occidentale* leaves extract. *Saudi Journal of Biological Sciences*, 26(3), 455–459. <https://doi.org/10.1016/j.sjbs.2018.12.001>
- Sutharsingh, R., Kavimani, S., Jayakar, B., Uvarani, M., & Thangathirupathi, A. (2011). Quantitative phytochemical estimation and antioxidant studies on aerial parts of *Naravelia zeylanica* DC. *International Journal of Pharmaceutical Studies and Research*, 2(2), 52–56.
- Tahir, K., Nazir, S., Li, B., Khan, A. U., Khan, Z. U. H., Gong, P. Y., Khan, S. U., & Ahmad, A. (2015). Nerium oleander leaves extract mediated synthesis of gold nanoparticles and its antioxidant activity. *Materials Letters*, 156, 198–201. <https://doi.org/10.1016/j.matlet.2015.05.062>
- Viuda-Martos, M., Ruiz-Navajas, Y., Fernández-López, J., & Pérez-Álvarez, J. A. (2011). Spices as functional foods. *Critical Reviews in Food Science and Nutrition*, 51(1), 13–28. <https://doi.org/10.1080/10408390903044271>
- Yoganandham, S. T., Ravindranath, R. R., Sathyamoorthy, G., Renuka, R. R., & Lakshminarayanan, A. (2018). Toxicity of biogenic AuNPs fabricated by *Hybanthus enneaspermus* aqueous extract against *Anopheles stephensi* and *Culex tritaeniorhynchus*. *Research Journal of Biotechnology*, 13, 26–34.
- Zahin, N., Anwar, R., Tewari, D., Kabir, M. T., Sajid, A., Mathew, B., Uddin, M. S., Aleya, L., & Abdel-Daim, M. M. (2020). Nanoparticles and its biomedical applications in health and diseases: Special focus on drug delivery. *Environmental Science and Pollution Research International*, 27(16), 19151–19168. <https://doi.org/10.1007/s11356-019-05211-0>

**Cite this article:** Sowmya KM, Narendhirakannan RT. Green Synthesis, Characterization and Bioactivity of AuNPs from *E. cardamomum*: A Comparative Study. *Int. J. Pharm. Investigation*. 2025;15(2):417-33.